

# Pure spin current in graphene N S structures

D. Greenbaum,<sup>1</sup> S. Das,<sup>1</sup> G. Schwiete,<sup>1</sup> and P. G. Silvestrov<sup>2</sup>

<sup>1</sup>Department of Condensed Matter Physics, Weizmann Institute of Science, 76100 Rehovot, Israel

<sup>2</sup>Theoretische Physik III, Ruhr-Universität Bochum, 44780 Bochum, Germany

(Dated: April 15, 2024)

We demonstrate theoretically the possibility of producing a pure spin current in graphene by filtering the charge from a spin-polarized electric current. To achieve this effect, which is based on the recently predicted property of specular Andreev reflection in graphene, we propose two possible device structures containing normal-superconductor (NS) junctions.

PACS numbers: 74.45.+c, 73.23.-b, 85.75.-d, 81.05.Uv

## I. INTRODUCTION

The recent experimental realization of conducting two dimensional monolayers of graphite [1, 2, 3, 4], also known as graphene, offers the promise for new electronic devices. One conceivable use for graphene is in spintronics [5], where the lack of nuclear spin interaction (<sup>12</sup>C has no nuclear spin) could offer the ability to maintain spin coherence over larger distances than in conventional semiconductors. For progress towards this goal, it is essential to have simple and reliable means to transport spin in graphene.

We address this issue by proposing a prescription for producing a pure spin current in ballistic bulk graphene. Spin currents have already been predicted to arise in graphene due to spin-orbit coupling [6] and the Quantum Hall effect [7]. In both cases, the spin currents are due to counter-propagating edge states of opposite spin. Our proposal makes use of the recently predicted specularly [8] of Andreev reflection [9] in graphene to produce a pure spin current in bulk. This is accomplished using structures containing normal-superconducting (NS) boundaries, which filter the charge out of a current of spin-polarized quasiparticles, leaving behind a pure spin current. To be specific, we consider two device paradigms: 1) a V-junction geometry with opening angle appropriately tuned, 2) a channel with a superconductor at one boundary and a normal edge at the other. An advantage of such devices is the large number of transmitting channels in the bulk, offering the possibility of rapid spin accumulation. Also, our proposal does not require a magnetic field, nor does it rely on the spin-orbit gap. In the present case, however, it is crucial to first generate a spin-polarized electric current, which could conceivably be done by contacting the system to a ferromagnetic lead, as has been done with carbon nanotubes [10].

Our description of proximity effects in graphene follows that of Ref. [8]. Later publications, Refs. [11, 12], used this approach to discuss the Andreev spectrum and Josephson effect in NS (SNS) structures in graphene. A very recent paper [13] makes explicit use of the specularly of Andreev reflection in graphene by considering the neutral excitations propagating along a narrow SNS channel. These authors propose a device that is similar to

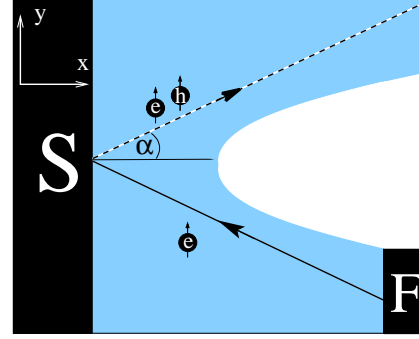


FIG. 1: V-junction with NS interface. Polarized electrons are injected through the lower arm and the same polarization is transferred to the upper arm by the electron-hole beam.

the one considered below in Sec. IV, but suggest investigating the thermoelectric effect to observe the chargeless excitations. In contrast, we analyze the spin transport. Our approach also lends itself to an analysis of the deviations from perfect charge filtering in a channel, which is done in Sec. V. Finally, an elegant method to produce pure spin currents in conventional semiconductors was suggested in Ref. [14], where the spatial separation of electron and hole trajectories is caused by tunneling through a superconductor.

## II. ANDREEV REFLECTION IN GRAPHENE

The electron wave function in graphene is described by a two component (pseudo-)spinor. Its spin-up and spin-down components correspond to the quantum mechanical amplitudes of finding the particle on one of the two sublattices of the honeycomb lattice. The low energy physics of graphene is governed by two so-called Dirac points in the spectrum, located at the two inequivalent corners  $K$ ;  $K^0$  of the Brillouin zone. The spinor wave function for low energy excitations in (lightly-doped) graphene decomposes into a sum of two waves oscillating with different wave vectors  $\psi = e^{iK \cdot r} + e^{iK^0 \cdot r}$ . The smooth envelope functions satisfy the two-dimensional Dirac equation [15] described by the Hamiltonian

tonian

$$H = c(\mathbf{p}_x \mathbf{p}_x + \mathbf{p}_y \mathbf{p}_y) + U(\mathbf{x}); \quad (1)$$

where  $c$  is the Fermi velocity and  $\mathbf{p} = \hbar \mathbf{k}$ . In regions of constant  $U$  this equation defines a conical energy band, or valley,  $U = c|\mathbf{p}|$ . The Pauli matrices  $\sigma_{x,y}$  permute electrons between two triangular sublattices of the honeycomb lattice. The two signs in Eq. (1) (+) and (-) correspond to the two valleys  $K$  and  $K^0$ .

We consider a graphene sheet in the  $x$ - $y$  plane, with the region  $x < 0$  covered by a conventional superconductor (Fig. 1). Following Ref. [8] we assume that in this configuration a pair potential  $\Delta(x) = \Delta_0 \Theta(-x)$  can be induced [16] in the graphene sheet by the proximity effect, accompanied by a sufficiently strong shift in the scalar potential  $U(x) = U_0 \Theta(-x)$ , so that  $U_0 = \Delta_0$ . The reflection at the NS interface ( $x = 0$ ) is described by a separate four-dimensional Dirac-Bogoliubov-de Gennes equation [8] for each valley

$$H \begin{pmatrix} u \\ v \end{pmatrix} = E_F \begin{pmatrix} u \\ v \end{pmatrix} + \begin{pmatrix} \Delta(x) \\ 0 \end{pmatrix} \begin{pmatrix} u \\ v \end{pmatrix}; \quad (2)$$

where the two spinors  $u$  and  $v$  represent the electron and hole components of the wavefunctions for  $H$ , respectively.

In addition to carrying pseudo-spin, electron-hole, and valley indices, the quasiparticle wave function should also describe the usual spin. Since for  $\mu < 0$  no spin can be injected into the superconductor, the spin of the incident electron is transferred to the reflected particle.

For several decades it was considered a basic feature of Andreev reflection [9] that the hole produced upon electron-hole conversion retraces the incident electron's trajectory. Even in the traditional materials, however, this repetition of trajectories is exact only for zero excitation energy  $\mu$  in Eq. (2). At finite excitation energy the two trajectories do not quite coincide, leading to interesting effects in semiclassical dynamics [17] and the spectrum [18] of Andreev billiards. In graphene, the Andreev reflection described by Eq. (2) has the standard form only if  $\mu = E_F$ . Because of the possibility to tune the Fermi energy close to the Dirac point, one may reach in graphene the regime  $\mu = E_F$ , so that an incident electron in the conduction band produces an Andreev reflected hole in the valence band (opposite side of the cone in the Dirac excitation spectrum). This valence band hole has the same velocity along the NS interface as the incident electron, and consequently is specularly reflected [8]. For vanishing Fermi energy, both the electron and hole components of the reflected wave follow precisely the same trajectory. We now restrict ourselves to this most interesting case of  $E_F = 0$ .

The transformation of a quantum superposition of incident electron and hole into the corresponding superposition of outgoing waves upon Andreev reflection is

described by a 2 × 2 reflection matrix,  $R_A$ ,

$$\begin{pmatrix} u \\ v \end{pmatrix}_{\text{out}} = R_A \begin{pmatrix} u \\ v \end{pmatrix}_{\text{in}} = \begin{pmatrix} r & r_A \\ r_A & r \end{pmatrix} \begin{pmatrix} u \\ v \end{pmatrix}_{\text{in}}; \quad (3)$$

With the notation  $\theta = \arctan(p_y/p_x)$ ,  $\mu = c \sqrt{p_x^2 + p_y^2}$ , and  $\mu = \frac{p}{\mu_0}$  one has [19]

$$r = \frac{i\mu \sin \theta}{\mu + i \cos \theta}; \quad r_A = \frac{\mu_0 \cos \theta}{\mu + i \cos \theta}; \quad (4)$$

### III. NS INTERFACE IN V-JUNCTION GEOMETRY

Characteristic of specular Andreev reflection in graphene is the spatial separation of incident and reflected electron-hole beams. The simplest device that makes use of this property is a V-junction, as shown in Fig. 1. Suppose one can inject a spin-polarized collimated monoenergetic beam of electrons through one arm of the junction. Monoenergetic beams may potentially be produced by resonant transport through a graphene quantum dot (QD) [20], as was done for semiconductor QD's e.g. in Ref. [21]. The injected electron will be either normally or Andreev reflected at the NS interface and the created quasiparticle will escape through the second arm. Since no spin can penetrate through the superconductor, all the polarization of the injected beam is transferred to the second arm. On the other hand, the average charge of the quasiparticles reflected towards the second arm depends on the excitation energy. One obtains zero reflected total charge by setting  $\theta_j = \frac{\pi}{4}$ . This constrains the incident particle energy to be

$$\mu = \mu_0 \cot \theta; \quad (5)$$

Alternatively, one may consider the injection of a collimated beam of electrons with all possible energies in the range  $0 < \mu < eV$ . For Dirac particles and a fixed angular spread of the beam, cancellation of the reflected charge requires

$$\int_0^{\theta_{\text{ev}}} \mu d\theta = \int_0^{\theta_{\text{ev}}} \mu_A d\theta; \quad (6)$$

One may think here about electrons leaving the biased ( $eV$ ) graphene half-plane through a narrow slit and then both angle- and width-collimated by a second slit. Substitution of Eq. (4) into Eq. (6) leads to the transcendental equation

$$\ln \left( 1 + \frac{eV}{\mu_0} \tan^2 \theta \right) = \frac{1}{2} \frac{eV}{\mu_0} \tan^2 \theta; \quad (7)$$

with the solution

$$eV = 1.59 \mu_0 \cot \theta; \quad (8)$$



lent. The charge per quasiparticle with incident angle  $\theta$  changes linearly along the channel from  $+e$  at  $y = 0$  to  $-e$  at

$$y = y_0 = 2W \tan \theta. \quad (13)$$

At  $y = y_0$  all electrons injected at angle  $\theta$  are converted to holes. At  $y_0 < y < 2y_0$  the holes are converted back to electrons. Charge here changes back (linearly) from  $+e$  to  $-e$ , and so on.

Figure 3 shows the average charge per quasiparticle for electrons injected at a fixed angle  $\theta$  at various initial positions,  $0 < x < 2W$ , as a function of  $p_x = \hbar k_x / m^* v_F$  for  $L = 10W$ . The segments of the function  $Q(p_x)$  are given by  $(n = 0; 1; 2; \dots)$

$$Q(p_x) = e(-1)^n \frac{L}{W} \frac{c p_x}{(c p_x)^2 + (2n+1)^2} \quad (14)$$

Averaging (integrating) further over  $p_x$  and introducing a new variable  $\xi = c p_x / (2n+1)$ , we find the charge fraction  $\langle Q \rangle$  per quasiparticle remaining in the beam to be

$$\langle Q \rangle = \frac{e}{2} \int_{-1}^1 F(\xi) \frac{d\xi}{(1+\xi^2)^{3/2}}. \quad (15)$$

Here we have introduced the sawtooth function  $F(\xi) = \xi$  for  $|\xi| < 1$  and  $F(\xi) = \text{sgn}(\xi)$  for  $|\xi| > 1$ . Keeping only the first harmonic in the Fourier transform of  $F(\xi)$  in the integral in Eq. (15) gives

$$\langle Q \rangle = \frac{4e}{\pi} \frac{L}{W} \exp\left(-\frac{L}{2W}\right). \quad (16)$$

Remarkably, the corrections to charge neutrality are exponentially small in the limit  $L \gg W$ . Since this incomplete cancellation of charge is of geometric origin, Eq. (16) does not depend on the voltage bias  $eV$ .

Another source of incomplete charge filtering in the NS channel is the coexistence of Andreev and normal reflection for finite quasiparticle energies ( $\hbar v_F \ll E_F$ ). To

find the charge transfer in this case we add to the reflection matrix, Eq. (3), a part describing particle propagation in graphene between Andreev reflections

$$R = R_0 R_A. \quad (17)$$

The form of  $R_0$  is sensitive to the details of quasiparticle reflection at the normal side of the strip. Depending on the microscopic structure of the graphene edge, reflection from it may or may not introduce transitions between the two valleys  $K, K^0$ . Here we consider only the latter case as an example. This also means that  $R_0$  is a  $2 \times 2$  diagonal matrix.

In the case of decoupled valleys the boundary conditions may only have the form (see Ref. [25] for the general situation)

$$(a_1 + b_2)_{j=W} = 0; \quad a, b = \text{const} \quad (18)$$

where  $\psi_1$  and  $\psi_2$  are the up and down components of either the particle (u), or hole (v) wave function. Particle number conservation imposes certain restrictions on the allowed values of  $a$  and  $b$ . Below we consider two examples of such boundary conditions, demonstrating both existence and absence of corrections to charge filtering due to finite voltage.

1. The first option is  $a=b=i$  (for the edge along the  $y$  axis). This boundary is realized if the particle confinement is achieved by adding a term with large mass  $m^* c^2$  to the Dirac equation (1) at  $x > W$  [26, 27]. Straightforward calculation for such a boundary gives

$$R_0 = i e^{ip_x W} \sim \text{diag}(1; -1); \quad (R_0 R_A)^2 / I = \quad (19)$$

The particle-hole superposition produced upon Andreev reflection of an electron returns to the pure electron state after the second reflection from the superconductor. The expectation value of the quasiparticle charge along a given trajectory according to Eq. (19) switches from  $+e$  to  $(\psi_A^\dagger \psi - \psi^\dagger \psi_A)e$  and back after each reflection from the NS-interface. [The average charge of the beam with initial angle  $\theta$  now changes linearly between these two values, not between  $+e$  and  $-e$  as in Eqs. (14,15).] Averaging over angles and energy using the exact Eq. (4) gives the charge per quasiparticle transmitted through the graphene channel for  $eV \gg \hbar v_F$  as

$$\langle Q \rangle = \frac{eV}{3 \hbar v_F} e. \quad (20)$$

We note that according to Eq. (4) the condition  $\psi = \psi_A$  is violated for grazing trajectories, having  $\theta = 0$  (4). The small statistical weight of these grazing trajectories is the source of the small value of  $\langle Q \rangle$ .

The result Eq. (20) was found in the limit  $L \gg W$ . However, further increase of the channel length does not lead here to charge relaxation, in contrast with the geometric correction, Eq. (16). The possibility for finite charge current, Eq. (20), to flow without leaking along a (arbitrarily) long NS-interface is very counterintuitive.

2. The second possibility consistent with particle conservation Eq. (18) is  $a=b=0$  (i.e. either  $a=0$ , or  $b=0$ ). Boundary conditions of this type describe the bulk envelope functions in graphene with a zigzag edge [7]. Reflection from the normal edge is now described by a pure phase matrix  $R_0 = e^{i\phi} \text{diag}(1; 1)$ . Therefore the product of  $n$  reflections reduces to

$$(R)^n = (R_A)^n = I \cos n\theta + i \sigma_x \sin n\theta; \quad (21)$$

where  $\cot \theta = \tan \theta = 0$  and the matrix  $\sigma_x$  interchanges particles and holes. Eq. (21) leads to a uniform (to exponential accuracy, as in Eq. (16)) mixing of particles and holes after many reflections at the channel boundaries for any value of  $\theta$ , i.e. at any  $\theta < \pi/2$ . In contrast to the previous example, the charge per quasiparticle transmitted through the graphene channel for  $L \gg W$  is zero even at finite values of  $\theta = 0$ .

## VI. CONCLUSIONS

In summary, we have proposed two basic device concepts for conversion of polarized electric current into pure spin current in ballistic bulk graphene. The second device, where the filtering of charge originates simply from the equilibration of the number of trajectories experiencing an even or odd number of Andreev reflections, seems especially promising. We expect this idea to be easily generalized beyond ballistic transport and for different geometries. We stress that neither proposal requires a 100% polarization of the incident beam, although the spin transfer rate will of course depend on the initial polarization.

## Acknowledgements

DG, SD and GS acknowledge stimulating discussions with Y. Oreg, and PGS acknowledges discussions with A.R. Akhmerov. In addition, SD thanks V. Falko and A. Imamoglu for discussions, and S. Rao for useful comments. DG, SD and GS were supported by the Feinberg Fellowship program at WIS. PGS was supported by the SFB TR 12, and his visit at Weizmann was supported by the EU-Transnational Access program, EU project RITA-CT-2003-506095.

- 
- [1] K.S. Novoselov, A.K. Geim, S.V. Morozov, D. Jiang, Y. Zhang, S.V. Dubonos, I.V. Grigorieva, and A.A. Firsov, *Science*, 306, 666 (2004)
- [2] K.S. Novoselov, A.K. Geim, S.V. Morozov, D. Jiang, M.J. Katsnelson, I.V. Grigorieva, S.V. Dubonos, and A.A. Firsov, *Nature* 438, 197 (2005).
- [3] Y. Zhang, Y.-W. Tan, H.L. Stormer, and P. Kim, *Nature* 438, 201 (2005).
- [4] C. Berger, Z. Song, X. Li, X. Wu, N. Brown, C. Naud, D. Mayou, T. Li, J. Hass, A.N. Marchenkov, E.H. Conrad, P.N. First, and W.A. de Heer, *Science* 312, 1191 (2006).
- [5] S.A. Wolf, D.D. Awschalom, R.A. Buhrman, J.M. Daughton, S. von Molnar, M.L. Roukes, A.Y. Chtchelkanova, D.M. Treger, *Science* 294, 1488 (2001).
- [6] C.L. Kane and E.J. Mele, *Phys. Rev. Lett.* 95, 226801 (2005).
- [7] D.A. Abanin, P.A. Lee, and L.S. Levitov, *Phys. Rev. Lett.* 96, 176803 (2006).
- [8] C.W.J. Beenakker, *Phys. Rev. Lett.* 97, 067007 (2006).
- [9] A.F. Andreev, *Sov. Phys. JETP* 19, 1228 (1964).
- [10] K. Tsukagoshi, B.W. A. Iphenaar, and H. Ago, *Nature* 401, 572 (1999).
- [11] M. Titov and C.W.J. Beenakker, *Phys. Rev. B* 74, 041401(R) (2006).
- [12] S. Bhattacharjee and K. Sengupta, *Phys. Rev. Lett.* 97, 217001 (2006)
- [13] M. Titov, A. Ossipov, and C.W.J. Beenakker, *Phys. Rev. B* 75, 045417 (2007)
- [14] N.M. Chtchelkatchev, *JETP Letters* 78, 230 (2003).
- [15] D.P. Divincenzo and E.J. Mele, *Phys. Rev. B* 29, 1685 (1984).
- [16] For a case of planar junction between a two-dimensional metal and a superconductor see: A.F. Volkov, P.H.C. M. Agnee, B.J. van Wees, and T.M. Klapwijk, *Physica C* 242, 261 (1995).
- [17] I. Kosztin, D.L. Maslov, and P.M. Goldbart, *Phys. Rev. Lett.* 75, 1735 (1995).
- [18] P.G. Silvestrov, M.C. Goorden, and C.W.J. Beenakker, *Phys. Rev. Lett.* 90, 116801 (2003); P.G. Silvestrov, *Phys. Rev. Lett.* 97, 067004 (2006).
- [19] The four plane-wave solutions in the normal region used to derive Eq. (4) are (up to normalization)
- $$(u;v)_e = (\exp(i=2); \exp(i=2); 0; 0);$$
- $$(u;v)_h = (0; 0; \exp(i=2); \exp(i=2));$$
- where (+) denotes  $p_x > 0$  and (−) denotes  $p_x < 0$ . More precisely, the R-matrix in Eqs. (3) and (4) denotes the transformation of a linear combination of incoming (−) electron and hole solutions into a superposition of outgoing (+) electron and hole solutions.
- [20] P.G. Silvestrov and K.B. Efetov, *Phys. Rev. Lett.* 98, 016802 (2007)
- [21] F. Hohls, M. Pepper, J.P. Grieths, G.A.C. Jones, and D.A. Ritchie, *Appl. Phys. Lett.* 89, 212103 (2006).
- [22] N.M. Peres, A.H. Castro Neto, and F. Guinea, *Phys. Rev. B* 73, 195411 (2006).
- [23] L. Brey and H.A. Fertig, *Phys. Rev. B* 73, 235411 (2006).
- [24] Since the accuracy of the calculation of the number of open channels, Eq. (11), is of order  $N^{-1}$ , the accuracy of this result is  $\propto \frac{1}{N} \propto \frac{e^2}{h} V$ . This estimate also includes the error due to the particles (holes) with energies close to the Dirac point,  $\epsilon \sim W$ , whose dynamics is not described by the geometric optics approximation.
- [25] E.M. McCann and V. Falko, *J. Phys.: Condens. Matter* 16, 2371 (2004).
- [26] M.V. Berry and R.J. Mondragon, *Proc. R. Soc. Lond. A* 412, 53 (1987).
- [27] J. Tworzydło, B. Trauzettel, M. Titov, A. Rycerz, and C.W.J. Beenakker, *Phys. Rev. Lett.* 96, 246802 (2006).